

Revealing the role of interfacial properties on catalytic behaviors by in situ surface-enhanced Raman spectroscopy

Hua Zhang,[†] Xia-Guang Zhang,[†] Jie Wei,[†] Chen Wang,[†] Shu Chen,[‡] Han-Lei Sun,[†] Ya-Hao Wang,[†] Bing-Hui Chen,^{*†} Zhi-Lin Yang,[‡] De-Yin Wu,[†] Jian-Feng Li,^{*†‡} and Zhong-Qun Tian[†]

[†]MOE Key Laboratory of Spectrochemical Analysis and Instrumentation, State Key Laboratory of Physical Chemistry of Solid Surfaces, iChem, College of Chemistry and Chemical Engineering, and [‡]Department of Physics, Research Institute for Biomimetics and Soft Matter, Xiamen University, Xiamen 361005, China

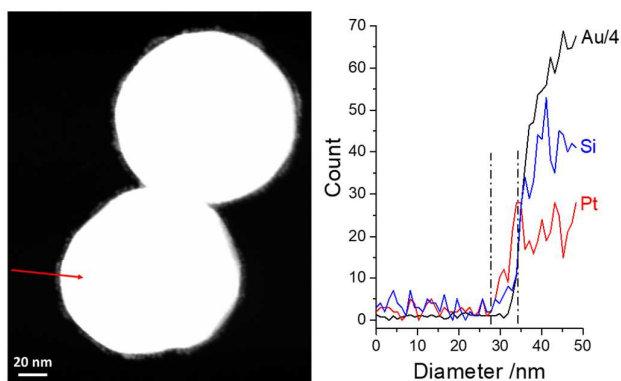


Figure S1. elemental line scan analysis of Pt-on-SHINs.

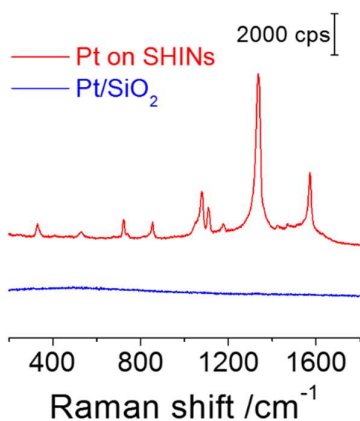


Figure S2. Raman spectra of pNTP adsorption on Pt-on-SHINs and Pt/SiO₂

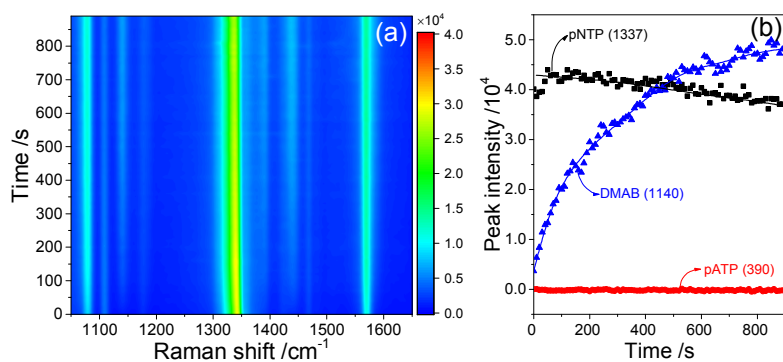


Figure S3. *In-situ* SERS spectra of the hydrogenation of pNTP on SHINs (a) and the corresponding intensity of pNTP, DMAB, and pATP as a function of reaction time (b).

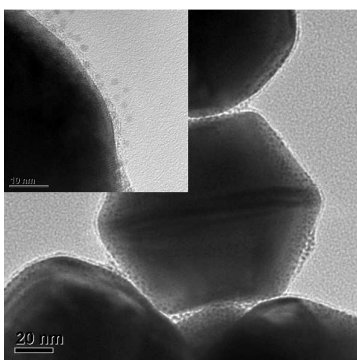


Figure S4. HR-TEM images of Pt-on-SHINs after reaction.

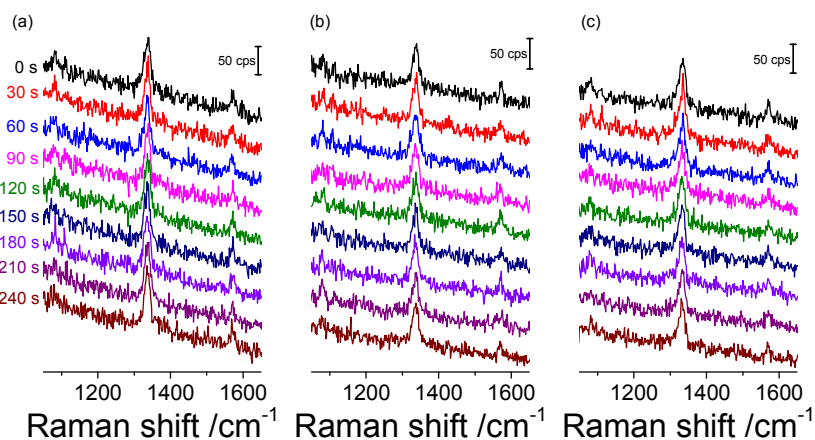


Figure S5. *In-situ* SERS spectra of the conversion of pNTP on pinhole-free SHINs under different conditions. (a) 25 °C, Ar. (b) 60 °C, Ar. (c) 60 °C, H₂. The intensities of the Raman signals for pNTP on the pinhole-free SHINs are much lower than those on Pt-on-SHINs (pinhole-free) due to the weak adsorption of pNTP on silica.

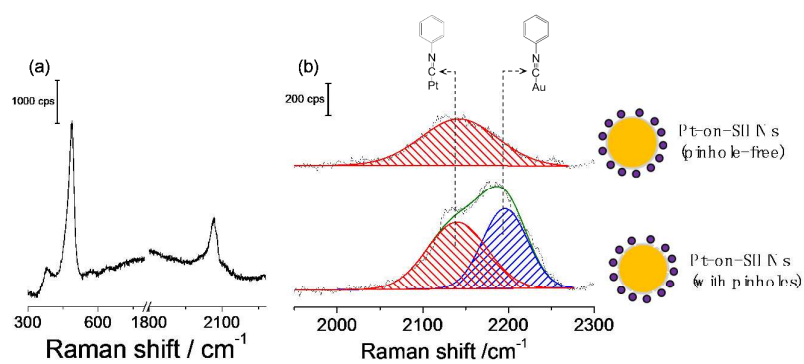


Figure S6. In situ SHINERS spectra of CO (a) and phenyl isocyanide (b) adsorbed on Pt-on-SHINs (pinhole-free)

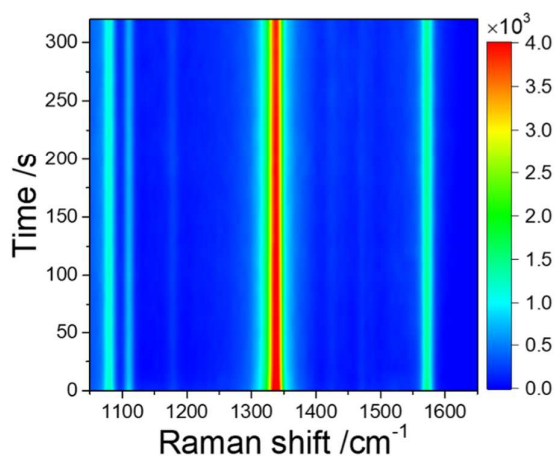


Figure S7. In-situ SERS spectra of the conversion of pNTP on Pt-on-SHINs (pinhole-free) under Ar at 60 °C.

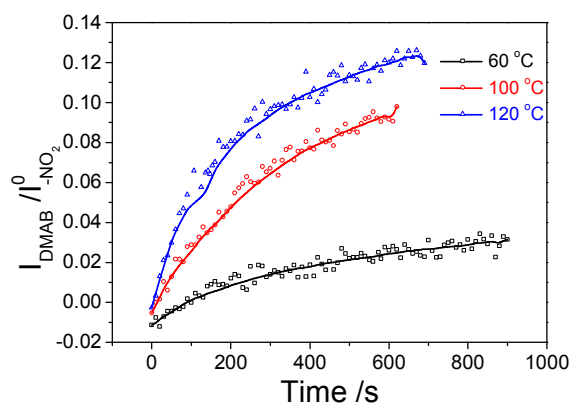


Figure S8. Effect of temperature on the yield of DMAB on Pt-on-Au via the photo-induced coupling reaction under Ar.

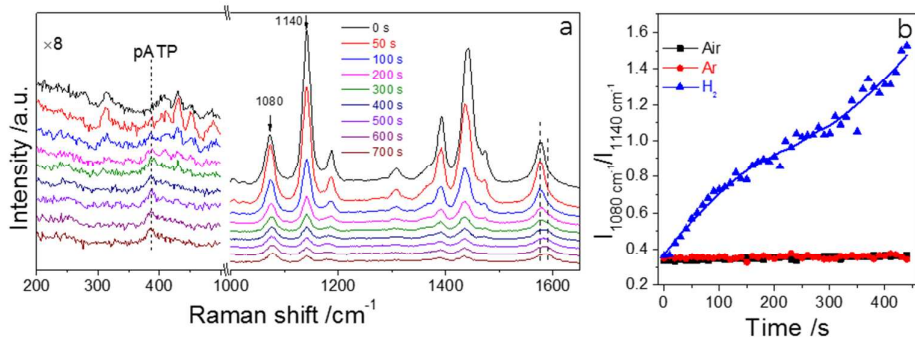


Figure S9. (a) In situ SERS spectra of the hydrogenation of DMAB on Pt-on-Au. It can be clearly seen that DMAB can be efficiently converted to pATP. (b) The ratio of the Raman band at 1080 cm^{-1} to that at 1140 cm^{-1} under different gaseous atmosphere as a function of time. Both DMAB and pATP show a strong Raman band at 1080 cm^{-1} , but only DMAB show a Raman band at 1140 cm^{-1} . Thus, the formation of pATP can also be speculated based on the ratio of the Raman band at 1080 cm^{-1} to that at 1140 cm^{-1} . This ratio only increases under H_2 , and maintains unchanged under Ar and air. It indicates the conversion of DMAB to pATP is triggered by H_2 rather than the laser.

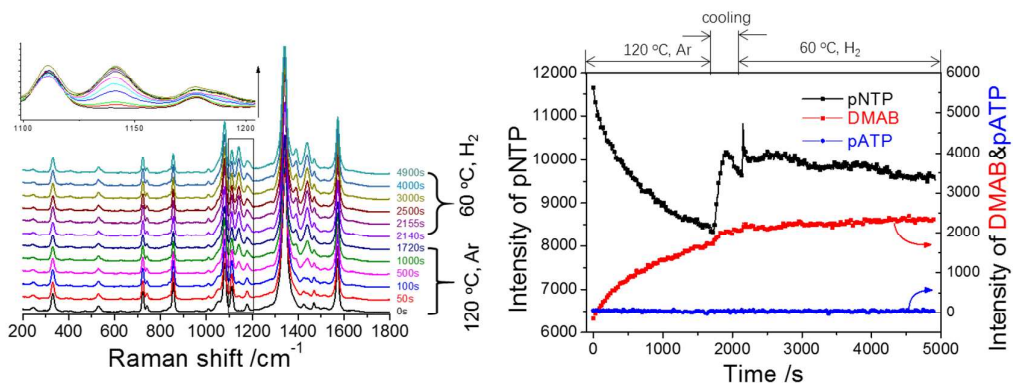


Figure S10. In situ SERS spectra of pNTP adsorbed on bare Au nanoparticles under Ar and H_2 .

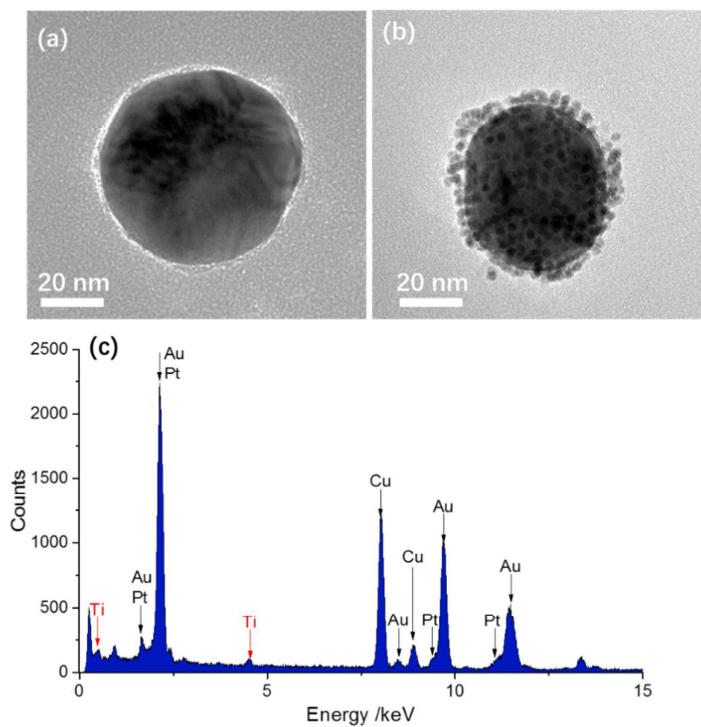


Figure S11. TEM image of SHINs with a TiO₂ shell (a) and the nanocomposite of Pt nanocatalysts on this kind of SHINs (Pt-on-SHINs (TiO₂ shell)) (b). (c) Energy dispersive spectroscopy (EDS) of the nanocomposites. Pt nanocatalysts are highly dispersed on the surface of the SHINs. The EDS analysis demonstrates that the shells are composed of TiO₂.